

# Reconstruction of the sedimentary structure and subsidence of the Congo Basin using geophysical data and numerical models

F.Maddaloni<sup>1</sup>, D.Delvaux<sup>2</sup>, J.Munch<sup>3</sup>, M.Tesauro<sup>1,4</sup>, T.Gerya<sup>3</sup>, C.Braitenberg<sup>1</sup>  
<sup>1</sup> Dept. of Mathematics and Geosciences, University of Trieste, Trieste, Italy;

<sup>2</sup>Royal Museum of Central Africa, Tervuren, Belgium; <sup>3</sup>Institute of Geophysics, ETH-Zurich, Zurich, Switzerland, <sup>4</sup> Dept. of Earth Sciences, Utrecht University, Utrecht, Netherlands

## 1. ABSTRACT

The Congo basin (CB) occupies a large part of the Congo Craton (1.2 million km<sup>2</sup>) covering approximately 10% of the continent. It contains up to 9 km of sedimentary rocks from Mesozoic until Quaternary age. The formation of the CB started with a rifting phase during the amalgamation of the Rodinia supercontinent at ~ 1.2 Gyr and the main episodes of subsidence occurred during the following post-rift phases in the Neoproterozoic and Paleozoic, separated by late Pan-African compressional inversion [1]. After a new compressional inversion at the end of the Permian, sedimentation resumed during the Mesozoic; since Cretaceous, the CB has been subjected to an intraplate compressional setting due to ridge-push forces related to the spreading of the South Atlantic Ocean [1].

In this study we first interpreted the seismic reflection profiles and well logs data located inside the central area of the CB, to reconstruct the stratigraphy/tectonic evolution of the basin. Afterwards, we compared geological and geophysical information to estimate the velocity, density, thickness of the sedimentary layers and the depth of the lithostratigraphic units. The results have been used as input parameters for a 3D numerical simulations, testing the main mechanisms of formation and evolution of the CB. To study this, we used the 3D thermomechanical code I3ELVIS [2] to simulate the initial rift phases. For the first experiments, we assumed that the Congo craton is made of four blocs of Archean age. We applied extensional stresses in the N-S and E-W directions (orthogonal stresses) [1] to test the hypothesis of the formation of a multi extensional rift in a cratonic area. The results of these first numerical experiments show that the deformation is localized in the central part of the CB.

- [1] De Wit, M.J., Stankiewicz, J., Reeves, C.V., (2008), Restoring Pan-African-Brasiliano connections: more Gondwana control, less Trans Atlantic corruption, 294, 10.1144/SP294.20, Geological Society, London, Special publications.  
 [2] Gerya, T., Introduction to numerical geodynamic modelling, Cambridge University Press. T. Gerya 2009.

## 2. INTERPRETATION OF SEISMIC REFLECTION PROFILES

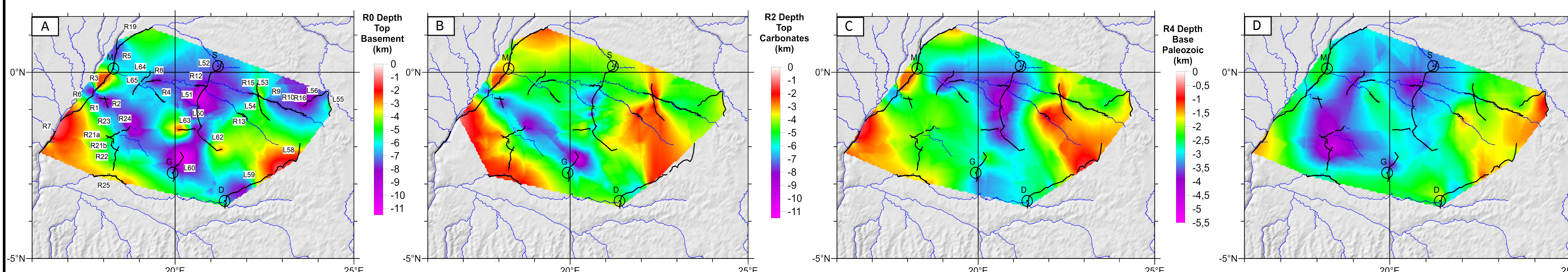


Fig.1 [A-D]: Depth of the main stratigraphic units. Black lines and circles show the location of the seismic reflection profiles and four boreholes, respectively.

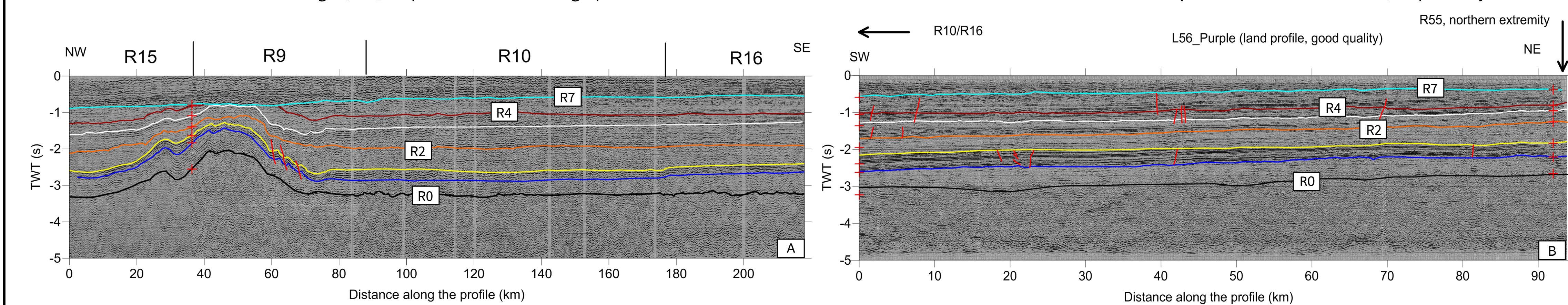


Fig.2 [A-B]: Two examples of interpreted seismic reflection lines. Profile A is the combination of R15-R9-R10-R16. Profile B corresponds to seismic line L56.

Legend for Figure 2:  
 - Top Basement (Mesoproterozoic): Black line  
 - Rift clastics (Mesoproterozoic): Blue line  
 - Dolostones (Meso-Neoproterozoic): Yellow line  
 - Top of the Carbonates (Neoproterozoic): Orange line  
 - Panafrican Unc. (Neoproter./Paleozoic): Grey line  
 - Redbeds (Paleozoic): Red line  
 - Base Jurassic Unc.: Light blue line  
 - Faults: Red dashed line

## 3. TECTONIC EVOLUTION

| Stratigraphic Periods / Era                | Seismic reflectors & sequences (Kadima et al., 2015)              | Units  | Tectonic / depos. context                                      | Density | Age max | Age min |
|--|---|--|--|---------|---------|---------|
| Cenozoic                                   | Seq 6: Subsurface   | Silicretes, laterites, aeolian deposits                          |  |         | 55      | 0       |
|  | Denudation 1-2 km in Samba & Dekese wells, normal faults in Kasal |  |  |         | 94      | 55      |
| Cenomanian - Turonian                      |   | Kwango   | Lacustrine, fluvial  |         | 1,87    | 110     |
|  | Seq 5b: Cretaceous  | Thrust faulting in Samba well                                    |  |         | 110     |         |
| Late Albian                                |   | Bokungu  | Fluvio-deltaic   |         | 2,05    | 110     |
| Late Aptian - Early Albian                 |   | Lola   | Fluvial, aeolian, ephemeral lakes                              |         | 2,09    | 132     |
| Kimmeridgian - Barremian - Valangian       | Seq 5a: Jurassic  | Stanleyville   | Fluvial-aeolian, shallow lacustrine                            |         | 2,14    | 157     |
|  | Hiatus  | Base Jurassic unconformity                                       | Regional erosion   |         | 200     | 157     |
| Triassic                                   |   | Haute Lueki  | Continental, warmer and dryer                                  |         | 2,29    | 250     |
| Hiatus                                     |   | Permo-Triassic unconformity                                      | Far-field compressional deform.                                |         | 250     |         |
| P/T  |   | Karoo  | Glacio-lacustrine  |         | 2,25    | 320     |
| Late Carb. - Permian                       |   | Congo basin at South pole  | Regional erosion   |         | 380     | 320     |
| Late Devonian - Early Carb. glacial period |   | Red Beds   | Syn-depositional extension                                     |         | 2,39    | 380     |
| Mid-Paleozoic?                             | Seq 4b: Red Beds  |  |  |         | 2,46    | 530     |
| Early Paleozoic?                           | Seq. 4a: ??   |  | Post-orogenic molassic deposits (Aruwimi-Inhisi - Kundelungu?) |         | 2,46    | 530     |
| Pan-African deformation                    |   | Pan-African regional unconformity                                | Folding (amalgamation against Congo Craton)                    |         | 530     |         |
| Neo-proterozoic                            | Seq. 3  | Banded seismic pattern, slightly divergent continuous reflectors | Siliciclastics   |         | 2,48    |         |
|  | Seq. 2  | Transparent seismic pattern with some continuous reflectors      | Carbonates-Evaporites-Clastics                                 |         | 2,61    |         |
|  | Seq. 1: Dolostones  | Mbuji-Mayi BII dolostones capped by lavas                        | Carbonate ramp in restricted marine rift basin                 |         | 2,75    | 1040    |
| Meso-proterozoic                           | Seq. 0: Rift clastics   | low amplitude discontinuous transparent seismic pattern          | Syn-rift, in mobile belt                                       |         | 2,62    | 1065    |
|  |   | Top crystalline basement unconformity                            |  |         |         |         |
| Paleo-Meso-proterozoic                     |   | Top basement   | Acoustic crystalline basement                                  |         |         |         |
|  |   | Basement   | Mobile belts & Archean cores                                   |         |         |         |

Table 1. Major tectonic events of the Congo basin from Archean to Cenozoic period. Colored circles refer to the main seismic horizons (Fig. 2).  
 References: [1] ESSO Zaire SARL (1981a) Geological completion report. Unpublished report; [2] Kadima EK (2007) Stratigraphie, structure géologique et prospective pétrolière du Bassin de la Cuvette congolaise; [3] Petroleum potential of the Congo Basin-Delvaux, M Fernandez-Alonso-Geology and Resource Potential of the Congo Basin, 2015; [4] Linol B (2013) Sedimentology and sequence stratigraphy of the Congo and Kalahari basins of South-Central Africa and their evolution during the formation and breakup of West-Gondwana. PhD thesis.

## 4. GRAVITY MODELS

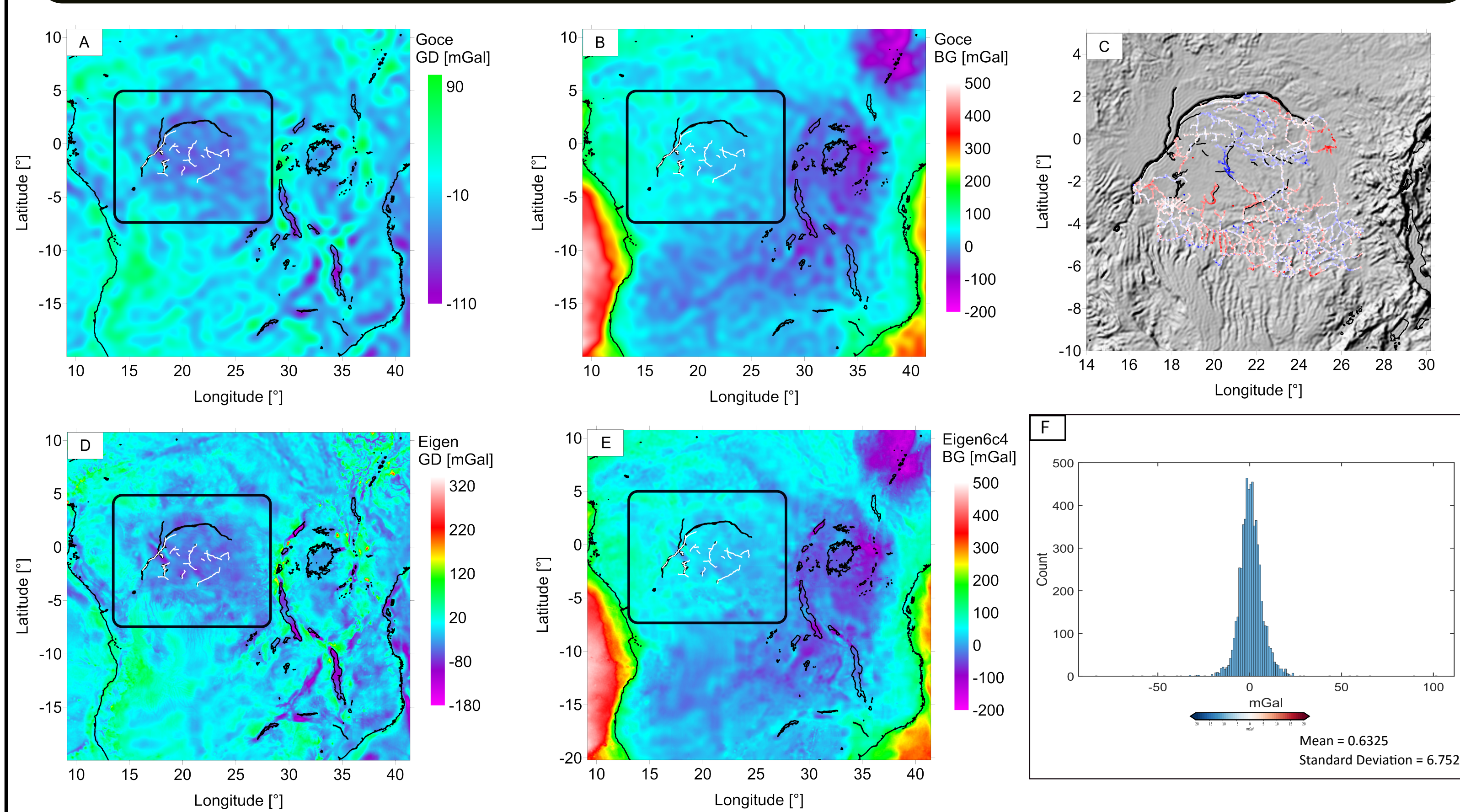
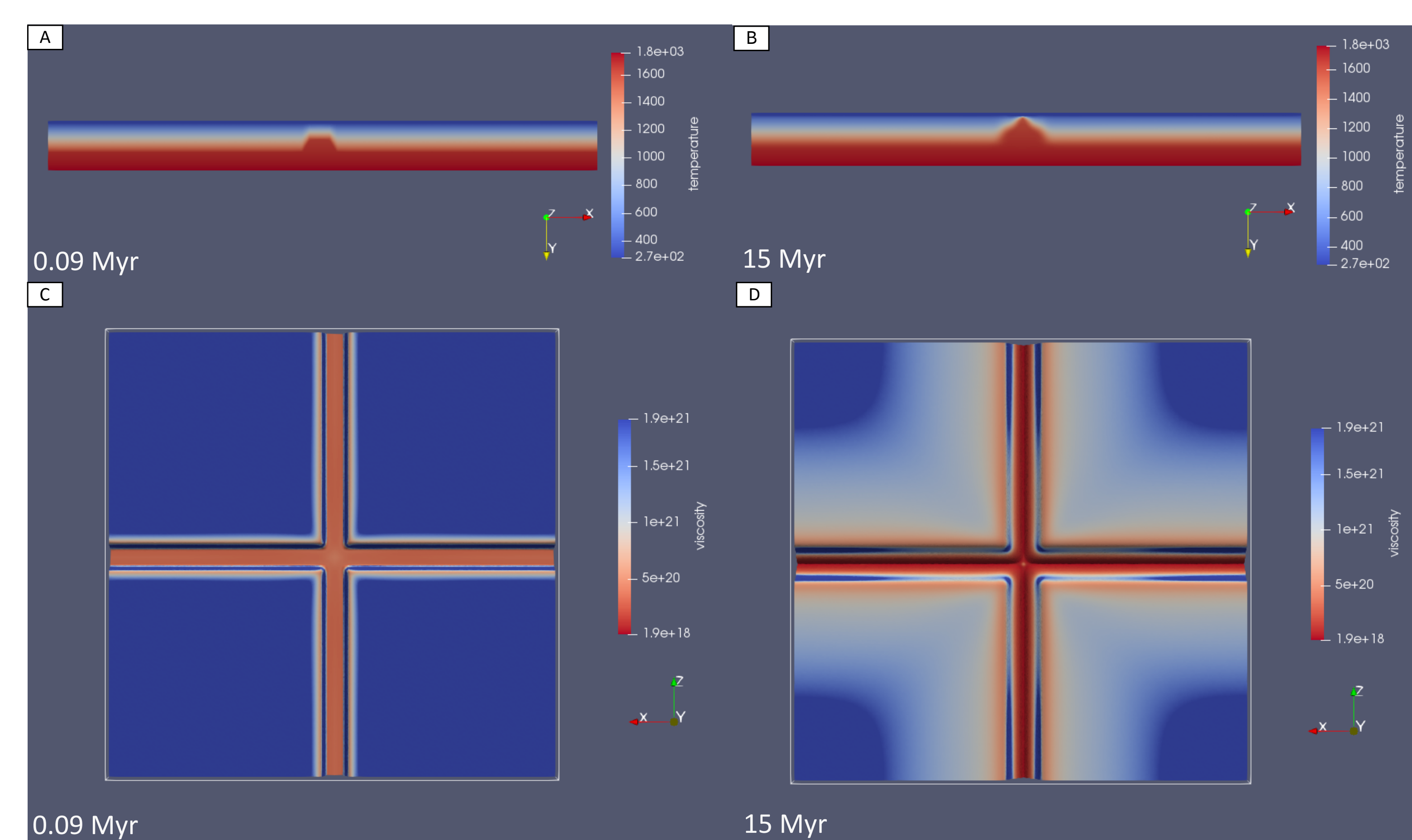


Fig.3 [A,B,D,E]: Gravity disturbance (GD) and Bouguer disturbance field maps estimated from GOCE (GO\_CONS\_GCF\_2\_TIM\_R5, maximum spherical harmonic degree: 280; grid resolution: 0.25) and Eigen (Eigen 6c4, maximum spherical harmonic degree: 2190, grid resolution: 0.05) gravity models. Eigen-6c4 contains the complete data of the GOCE mission, combined with those of LAGEOS, GRACE and Terrestrial data. [C]: Topography map. The model used is Etopo1 (maximum spherical harmonic degree: 2250, grid resolution: 0.05, <http://icgem.gfz-potsdam.de/ICGEM/>, 2008). Over the topography, the differences between the GD calculated using the Terrestrial data and Eigen-6c4 model are displayed. The histogram of residuals [F] shows a good agreement between the Terrestrial data and Eigen 6c4 model.  
 From the GD we identify two types of anomalies (Black boxes): one with a long wavelength that covers the entire area of the Congo basin and a second one with a short wavelength, having a NW-SE trend, which corresponds to the main depocenters of sediments (see the interpretation of the seismic reflection profiles in Fig. 1 A-D).

## 5. NUMERICAL MODELS



The 3D thermomechanical I3ELVIS is based on the conservation of mass, momentum and energy. It uses a visco plastic rheology and is based on a finite difference approach using a staggered grid and the markers in cells technique. The mechanical equation of momentum and mass is solved for a compressible non-Newtonian-visco-plastic fluid. The 3D computational domain covers 4050 km x 392 km with the resolution of 405 nodes for 4050 km: 10 km horizontal resolution, same for the vertical one with 2 km resolution. The tests have been conducted dividing the area into four cratonic blocks of size 1000 km x 1000 km, subjected to multi extensional stresses in orthogonal directions (N-S, E-W). Each craton moves in both directions 5 cm/yr. On the top, there is a layer of sticky air of 20 km of thickness. The vertical size of the cratonic blocks and area off-cratons is 250 and 150 km, respectively. The Moho depth is located at 55 km. All boundaries are free-slip. The thermal distribution of the continental lithosphere is calculated following a linear increase from 273K at the surface to 1698 K at the base of the cratonic blocks and to 1648 K at the base of the area off-cratons.  
 Fig.4 [A-B] Cross-section of the temperature distribution at the time step 0.09 Myr (A) and 15 Myr (B). We can observe the uplift of the asthenosphere in the central part of the area, due to the extensional stresses (B). [C-D] Lateral variation of viscosity in the upper mantle at the time step 0.09 Myr (C) and 15 Myr (D). We can observe a progressive weakening from the center to the corners of the area, in response to the extensional stresses.